The American Journal of
PATHOLOGY

GASTROINTESTINAL, HEPATOBILIARY, AND PANCREATIC PATHOLOGY

The Thyromimetic Sobetirome (GC-1) Alters Bile Acid Metabolism in a Mouse Model of Hepatic Cholestasis

Check for updates

Karis Kosar,* Pamela Cornuet,* Sucha Singh,* Silvia Liu,*[†] and Kari Nejak-Bowen*[†]

From the Department of Pathology* and the Pittsburgh Liver Research Center,[†] University of Pittsburgh, Pittsburgh, Pennsylvania

Chronic cholestasis results from bile secretory defects or impaired bile flow with few effective medical therapies available. Thyroid hormone triiodothyronine and synthetic thyroid hormone receptor agonists, such as sobetirome (GC-1), are known to impact lipid and bile acid (BA) metabolism and induce hepatocyte proliferation downstream of Wnt/β-catenin signaling after surgical resection; however, these drugs have yet to be studied as potential therapeutics for cholestatic liver disease. Herein, GC-1 was administered to ATP binding cassette subfamily B member 4 ($Abcb4^{-/-}$; $Mdr2^{-/-}$) knockout (KO) mice, a sclerosing cholangitis model. KO mice fed GC-1 diet for 2 and 4 weeks had decreased serum alkaline phosphatase but increased serum transaminases compared with KO alone. KO mice on GC-1 also had higher levels of total liver BA due to alterations in expression of BA detoxification, transport, and synthesis genes, with the net result being retention of BA in the hepatocytes. Interestingly, GC-1 does not induce hepatocyte proliferation or Wnt/β-catenin signaling in KO mice, likely a result of decreased thyroid hormone receptor β expression without Mdr2. Therefore, although GC-1 treatment induces a mild protection against biliary injury in the early stages of treatment, it comes at the expense of hepatocyte injury and is suboptimal because of lower expression of thyroid hormone receptor β. Thus, thyromimetics may have limited therapeutic benefits in treating cholestatic liver disease. *(Am J Pathol 2020, 190: 1006−1017; https://doi.org/10.1016/j.ajpath.2020.01.015)*

Many chronic liver diseases have few to no medical therapies that are capable of halting or reversing disease progression, and the only life-extending treatment is orthotopic liver transplantation. Primary sclerosing cholangitis (PSC), a chronic cholestatic liver disease of unknown etiology, is one such example. Patients with PSC have bile duct inflammation and fibrosis, which results in end-stage liver disease and reduced life expectancy.[1,2] A significant number (40%) of PSC patients will ultimately require liver transplant and up to 25% of patients who receive liver transplant will have recurrent PSC.[3] Therefore, an effective therapeutic strategy to treat PSC is a major unmet clinical need.

ATP binding cassette subfamily B member 4 ($Abcb4^{-/-}$; $Mdr2^{-/-}$) gene knockout (KO) mice spontaneously develop sclerosing cholangitis characterized by pericholangitis, ductular proliferation, and onionskin-type periductal fibrosis.[4] This phenotype is due to lack of the Mdr2 gene, a canalicular flippase that transports phospholipids into bile.[5] The loss of protective phospholipids in the KO leads to increased concentrations of free toxic bile acids (BAs), which damages cholangiocytes and causes bile to leak into the parenchyma.[6] Because the resulting liver injury resembles PSC, these mice have long been used to study the pathogenesis and signaling pathways involved in this disease, as well as to test potential therapeutics.

The Wnt/β-catenin signaling pathway has a well-described role in liver physiology and pathology, and its modulation

also alters the progression of cholestatic liver disease.[7] Loss or inhibition of β-catenin (alias catenin β 1) leads to improved outcomes after bile duct ligation and 5-diethoxycarbonyl-1,4-dihydrocollidine, two commonly used animal models of cholestasis.[8,9] However, it was recently shown that knockdown of β-catenin in Mdr2 KO leads to increased inflammation, oxidative stress, fibrosis, and impaired hepatocyte proliferation.[10] In this case, β-catenin is essential in maintaining homeostasis in the absence of Mdr2, and its loss results in decompensation and increased injury. Thus, in some types of cholestatic conditions, such as those modeled by the Mdr2 KO mouse, activation of β-catenin may be advantageous by balancing ongoing injury with a robust regenerative response.

Thyroid hormones, such as triiodothyronine (T3), are known to have mitogenic effects in many organs, such as the liver, heart, and pancreas.[11,12] In hepatocytes, T3 increases proliferation in mice through interaction with thyroid hormone receptor β (alias TRβ).[11,13] This occurs in a β-catenin–dependent manner via the cAMP-dependent protein kinase A pathway, which, in turn, leads to phosphorylation of β-catenin at Ser675 and subsequent activation.[14,15] However, because T3 is not liver specific, use of a selective TRβ agonist, such as GC-1 or sobetirome, is preferable because of its lack of off-target effects.[16] GC-1 is also well studied in the liver and has been shown to recapitulate the mitogenic effects of T3, stimulating β-catenin–dependent hepatocyte proliferation after partial hepatectomy.[15] However, whether these drugs can induce proliferation and repair during cholestatic liver disease is unknown.

In this study, wild-type (WT) and Mdr2 KO mice were treated with a GC-1–containing diet to activate β-catenin in hepatocytes. It was hypothesized that activation of β-catenin in this model of cholestasis would induce compensatory proliferation that may provide protection against injury. The study results show that biliary injury is transiently decreased in Mdr2 KO mice on GC-1 diet compared with Mdr2 KO mice on normal diet. This decrease in biliary injury is likely due to a lack of BA export by the hepatocytes, which spares cholangiocytes but leads to increased hepatic injury due to toxic BA retention. Also, although hepatocyte proliferation is increased in Mdr2 KO mice, it is not further induced by GC-1, nor is β-catenin activated in KO with GC-1. This is because KO have decreased responsiveness to GC-1 because of lesser expression of thyroid receptor β. This study shows that dysregulation of receptor targets during chronic liver disease may affect drug efficacy, and that caution should be used when considering the use of repurposed drugs to treat cholestatic liver diseases.

Materials and Methods

Animal Model

All animal studies were performed in accordance with the guidelines of the Institutional Animal Use and Care Committee at the University of Pittsburgh School of Medicine (Pittsburgh, PA) and the NIH (Bethesda, MD; protocol number 17071066). Five-week–old Mdr2 ($^{-/-}$) KO mice in an FVB/NJ background (Jackson Laboratory, Bar Harbor, ME; stock number 002539) or WT littermate controls were fed standard mouse chow or GC-1/sobetirome-supplemented diet (5 mg/kg of diet, GC-1/sobetirome purchased from MedChem Express, Monmouth Junction, NJ; diet from Animal Specialties and Provisions LLC, Quakertown, PA) for up to 4 weeks. After the diet course was complete, mice were sacrificed, and blood serum and livers were collected. Livers were sectioned, fixed in 10% formalin, and processed for paraffin embedding or frozen in liquid nitrogen and stored at $-80°C$. For baseline, $n = 3$ mice per genotype. For 1-week GC-1 or normal diet, $n = 4$ WT, $n = 3$ WT + GC-1, $n = 4$ KO, and $n = 3$ KO + GC-1. For 2-week GC-1 or normal diet, $n = 5$ WT, $n = 8$ WT + GC-1, $n = 6$ KO, and $n = 7$ KO + GC-1. For 4-week GC-1 or normal diet, $n = 8$ WT, $n = 7$ WT + GC-1, $n = 9$ KO, and $n = 8$ KO + GC-1. For 12-week GC-1 or normal diet, $n = 4$ WT, $n = 3$ WT + GC-1, $n = 4$ KO, and $n = 3$ KO + GC-1.

Serum Biochemistry

At the time of sacrifice, blood was collected and serum was sent to the University of Pittsburgh Medical Center Clinical Chemistry laboratory for biochemical analysis of total and direct bilirubin, alkaline phosphatase (ALP), aspartate aminotransferase, and alanine transaminase.

Immunohistochemical Analysis

Paraffin-embedded liver tissues were divided into sections (4 μm thick). Sections were stained with hematoxylin and eosin or Picro-Sirius Red (Abcam, Cambridge, UK). Immunohistochemistry on paraffin-embedded sections was performed on mouse livers, as described elsewhere.[17] Primary antibodies used were anti–sex-determining region Y-box transcription factor 9 (Sox9) antibody (1:100; Abcam), anti–cytokeratin 19 (CK19) antibody (31 μg/mL; TROMA-III-S; Developmental Studies Hybridoma Bank, Iowa City, IA), and proliferating cell nuclear antigen antibody (PC10; 1:4000; Santa Cruz Biotechnology, Dallas, TX). Secondary antibodies were goat anti-rabbit, goat anti-rat, and donkey anti-goat (Chemicon, Temecula, CA), and were used at 1 to 400, and staining was detected with 3,3′-diaminobenzidine detection systems after incubation with the Avidin-Biotin Complex Kit (Vector Laboratories, Burlingame, CA). Apoptotic nuclei were detected by the terminal deoxynucleotidyl transferase-mediated dUTP nick-end labeling staining using the ApopTag Peroxidase kit (Millipore, Temecula, CA) at the University of Pittsburgh Department of Pathology's core immunohistochemistry laboratory. Images (1280 by 1024 pixels) were taken on an Olympus Provis scope (Olympus America, Center Valley, PA) at the Center for Biological Imaging at the University of Pittsburgh.

Sirius Red images were quantified using ImageJ Fiji version 2.0.0-rc-68/1.521 (NIH; *https://imagej.nih.gov/ij*).[18] Each image was split into red, green, and blue channels, from which the green channel was selected for optimal separation of staining. The staining was isolated by using threshold setting 0 for the upper level and 127 for the lower level, and the percentage of the stained area to the total image was measured. A total of five images per mouse liver ($n = 3$ mice) were quantified for each genotype.

CK19 images were quantified by splitting the image into red/green/blue channels with ImageJ Fiji, and then quantifying the blue channel using a threshold setting 0 for the upper level and 63 for the lower level. The percentage of the stained area to the total image was then calculated. A total of five images per mouse liver ($n = 3$ mice) were quantified for each genotype.

Quantification of proliferating cell nuclear antigen— and terminal deoxynucleotidyl transferase-mediated dUTP nick-end labeling—positive cells was performed by counting the number of positive hepatocytes per ×100 field. A total of five images per mouse liver ($n = 3$ mice) were quantified for each genotype.

Protein Extraction and Western Blot Analysis

Whole-cell liver lysates were prepared in radio-immunoprecipitation assay buffer containing fresh phosphatase and protease inhibitor cocktails (Sigma Aldrich, St. Louis, MO). Denatured proteins were separated on 10% SDS-PAGE gels and transferred to polyvinylidene difluoride membranes. Membranes were blocked using 5% nonfat dry milk or 5% bovine serum albumin in 0.1% Triton X-100 in Tris-buffered saline at room temperature for 1 hour and incubated at 4°C overnight with primary antibodies (diluted in 3% blocking media). The following primary antibodies were used: glyceraldehyde-3-phosphate dehydrogenase (GAPDH; 1:5000; Invitrogen, Carlsbad, CA), purified mouse anti—β-catenin (1:500; BD Biosciences, San Jose, CA), nonphosphorylated (active) β-catenin (Ser33/37/Thr41) (1:1000; Cell Signaling Technology, Danvers, MA), and phosphorylated β-catenin (Ser675; D2F1; 1:1000; Cell Signaling Technology). Membranes were washed three times for 15 minutes each in Tris-buffered saline before being probed with horseradish peroxidase—conjugated secondary antibodies (1:20,000 diluted in 3% blocking media; Santa Cruz Biotechnology) for 2 hours at room temperature. Membranes were washed three times for 15 minutes each in Tris-buffered saline and visualized using the Enhanced Chemiluminescence System (GE Healthcare, Little Chalfont, UK).

Quantitative Real-Time PCR

Total RNA was isolated from frozen liver tissue using Trizol reagent (Invitrogen). RT-PCR was performed as described elsewhere.[17] Real-time PCR was performed on a CFX96 TouchReal-Time PCR Detection System (Bio-Rad Laboratories, Hercules, CA) using SYBR Green (Thermo Fisher Scientific, Pittsburgh, PA). Changes in target mRNA were normalized to GAPDH mRNA for each sample, and P value is presented as fold change over the average from three normal livers. Three samples per each condition were assayed in triplicate. Primer sequences are provided in Table 1.

Table 1 Primers Used for Quantitative RT-PCR Analysis

Primer name	Sequence
PXR (forward)	5′–CCCATCAACGTAGAGGAGGA–3′
PXR (reverse)	5′–GGGGGTTGGTAGTTCCAGAT–3′
SHP (forward)	5′–TCTGCAGGTCGTCCGACTATTC–3′
SHP (reverse)	5′–AGGCAGTGGCTGTGAGATGC–3′
FXR (forward)	5′–CTTGATGTGCTACAAAAGCTGTG–3′
FXR (reverse)	5′–ACTCTCCAAGACATCAGCATCTC–3′
CAR (forward)	5′–GGAGGACCAGATCTCCCTTC–3′
CAR (reverse)	5′–ATTTCATTGCCACTCCCAAG–3′
NTCP (forward)	5′–CACCATGGAGTTCAGCAAGA–3′
NTCP (reverse)	5′–AGCACTGAGGGGCATGATAC–3′
Slco1b2 (forward)	5′–GATCCTTCACTTACCTGTTCAA–3′
Slco1b2 (reverse)	5′–CCTAAAAACATTCCACTTGCCATA–3′
MRP2 (forward)	5′–GCTTCCCATGGTGATCTCTT–3′
MRP2 (reverse)	5′–ATCATCGCTTCCCAGGTACT–3′
MRP3 (forward)	5′–TGAGATCGTCATTGATGGGC–3′
MRP3 (reverse)	5′–AGCTGCGAGCGCAGGTCG–3′
MRP4 (forward)	5′–TTAGATGGGCCTCTGGTTCT–3′
MRP4 (reverse)	5′–GCCCACAATTCCAACCTTT–3′
BSEP (forward)	5′–ACACCATTGTATGGATCAACAGC–3′
BSEP (reverse)	5′–CACCAACTCCTGCGTAGATGC–3′
Cyp7a1 (forward)	5′–TGGGCATCTCAAGCAAACAC–3′
Cyp7a1 (reverse)	5′–TCATTGCTTCAGGGCTCCTG–3′
Cyp3a11 (forward)	5′–CCACCAGTAGCACACTTTCC–3′
Cyp8b1 (forward)	5′–GCCCTTACTCCAAATCCTACCA–3′
Cyp8b1 (reverse)	5′–TCGCACACATGGCTCGAT–3′
Cyp27 (forward)	5′–TGCCTGGGTCGGAGGAT–3′
Cyp27 (reverse)	5′–GAGCCAGGGCAATCTCATACTT–3′
Cyp3a11 (reverse)	5′–TTCCATCTCCATCACAGTATCA–3′
Cyp2B10 (forward)	5′–CAATGGGGAACGTTGGAAGA–3′
Cyp2B10 (reverse)	5′–TGATGCACTGGAAGAGGAAC–3′
CK19 (forward)	5′–GACCTGGAGATGCAGATTGAG–3′
CK19 (reverse)	5′–GCTCCTCAGGGCAGTAATTT–3′
Sox9 (forward)	5′–CAGGCAAGAATTGGGCAAAG–3′
Sox9 (reverse)	5′–CCTCCCAACACGCAGTAAA–3′
HNF1β (forward)	5′–AACCAGCCGGGAAACAATGA–3′
HNF1β (reverse)	5′–CTCCCGACACTGTGATCTGC–3′
TRβ1 (forward)	5′–GGACAAGCACCCATCGTGAAT–3′
TRβ1 (reverse)	5′–CTCTGGTAATTGCTGGTGTGAT–3′
TRβ2 (forward)	5′–CCAGAGGTACACGAAGTGTGC–3′
TRβ2 (reverse)	5′–AGGTTTCCAGGGTAACTACAGG–3′

BSEP, bile salt export pump; CAR, constitutive androstane receptor; CK19, cytokeratin 19; Cyp, cytochrome P450; FXR, farnesoid X receptor; HNF1β, hepatocyte nuclear factor 1 homeobox B; NTCP, sodium-taurocholate cotransporting polypeptide; PXR, pregnane X receptor; SHP, small heterodimer partner; Slco1b2, solute carrier organic anion transporter family, member 1b2; MRP, multidrug resistance protein; Sox9, sex-determining region Y-box transcription factor 9; TRβ, thyroid hormone receptor β.

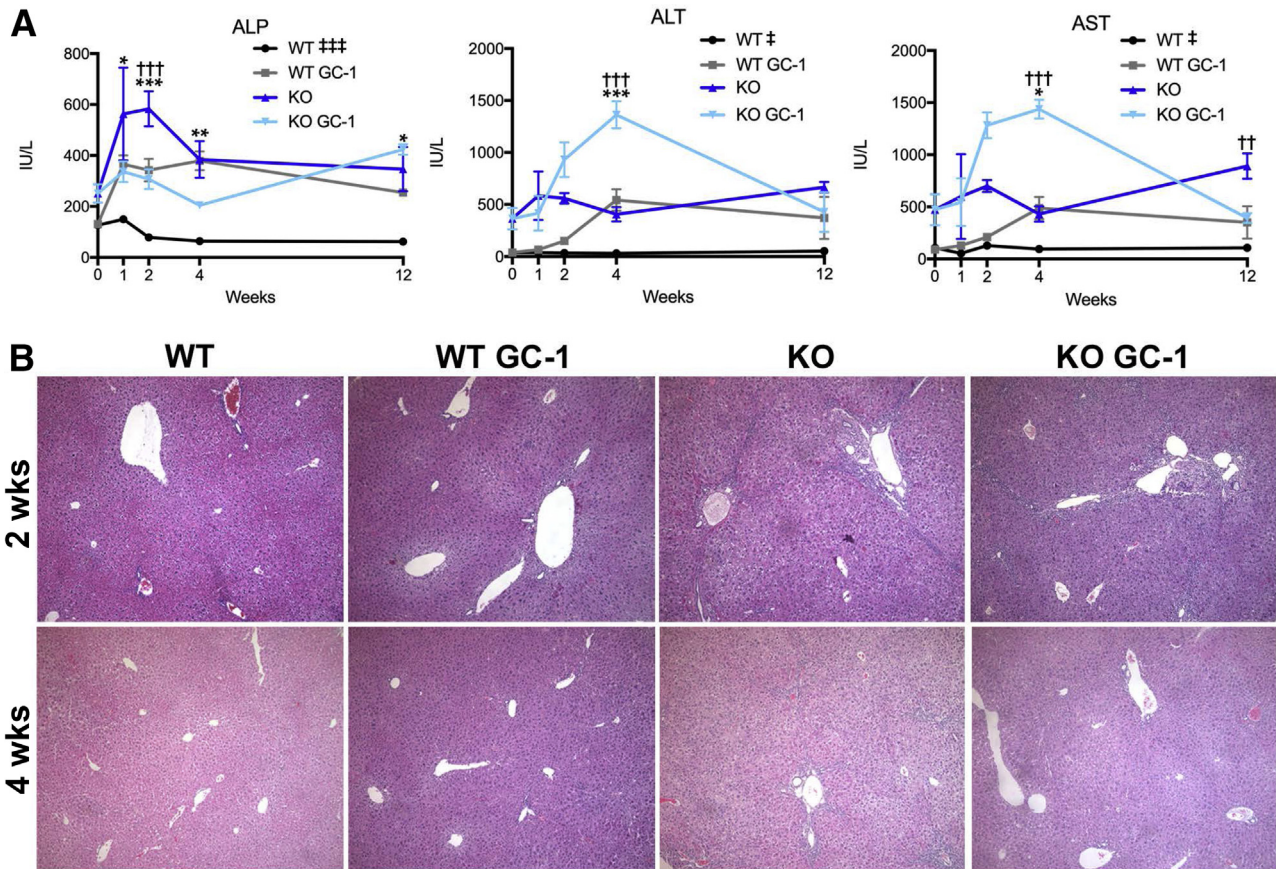**Figure 1** Biliary injury improves in ATP binding cassette subfamily B member 4 ($Abcb4^{-/-}$; $Mdr2^{-/-}$) knockout (KO) mice at 2 and 4 weeks after GC-1, at the expense of hepatic injury. **A:** Blood serum levels of alkaline phosphatase (ALP) show decreased biliary injury, whereas alanine aminotransferase (ALT) and aspartate aminotransferase (AST) indicate increased hepatic injury, in KO mice on short-term GC-1 diet compared with KO mice. **B:** Representative hematoxylin and eosin images show equivalent parenchymal injury in KO mice on GC-1 diet for 2 and 4 weeks compared with KO mice on normal diet. $n \geq 3$ mice per group (**A**). *$P < 0.05$, **$P < 0.01$, and ***$P < 0.001$ wild type (WT) versus WT GC-1; ††$P < 0.01$, †††$P < 0.001$ KO versus KO GC-1; ‡$P < 0.05$, ‡‡‡$P < 0.001$ WT versus KO at all time points analyzed. Original magnification, ×100 (**B**).

Measurement of BAs

Total BAs ($n = 3$ samples per condition) were isolated from frozen liver using 70% ethanol, as previously described.[8] Bile was also extracted from gallbladders and diluted 1:5 in distilled water. The Mouse Total Bile Acids Assay Kit (Crystal Chem, Downers Grove, IL) was used to measure BAs in both liver and bile, and the calibration curve and mean change in absorbance value for each sample were used to determine the concentration of each sample.

Statistical Analysis

Data are presented as means, SD, and/or individual data points. Data were analyzed, and graphs were generated using Prism GraphPad 7.0c (GraphPad Software, San Diego, CA). P values were determined using the two-tailed t-test, one-way analysis of variance followed by an appropriate post hoc test, or two-way analysis of variance followed by the appropriate post hoc test. $P < 0.05$ was considered statistically significant.

Results

Biliary Injury Is Decreased in KO after Short-Term GC-1 Diet

WT and KO mice were fed normal diet or GC-1 supplemented diet for 1, 2, 4, and 12 weeks and assessed for serum biochemical markers of liver injury. GC-1 diet did not affect total serum bilirubin levels nor liver weight/body weight ratios in KO mice, although conjugated bilirubin levels were decreased at 12 weeks (Supplemental Figure S1). Surprisingly, hepatic injury, as assessed by measurement of serum transaminases aspartate aminotransferase and alanine transaminase, was significantly increased in KO fed GC-1 as early as 2 weeks after the start of diet, although these numbers tended to normalize or decrease at 12 weeks (Figure 1A). Terminal deoxynucleotidyl transferase-mediated dUTP nick-end labeling staining also revealed increased hepatocyte death in KO + GC-1 treated livers at 2 and 4 weeks of diet (Supplemental Figure S2). On the contrary, biliary injury in KO mice on GC-1 diet was significantly decreased compared with KO mice on normal diet at both 2 and 4 weeks, as shown
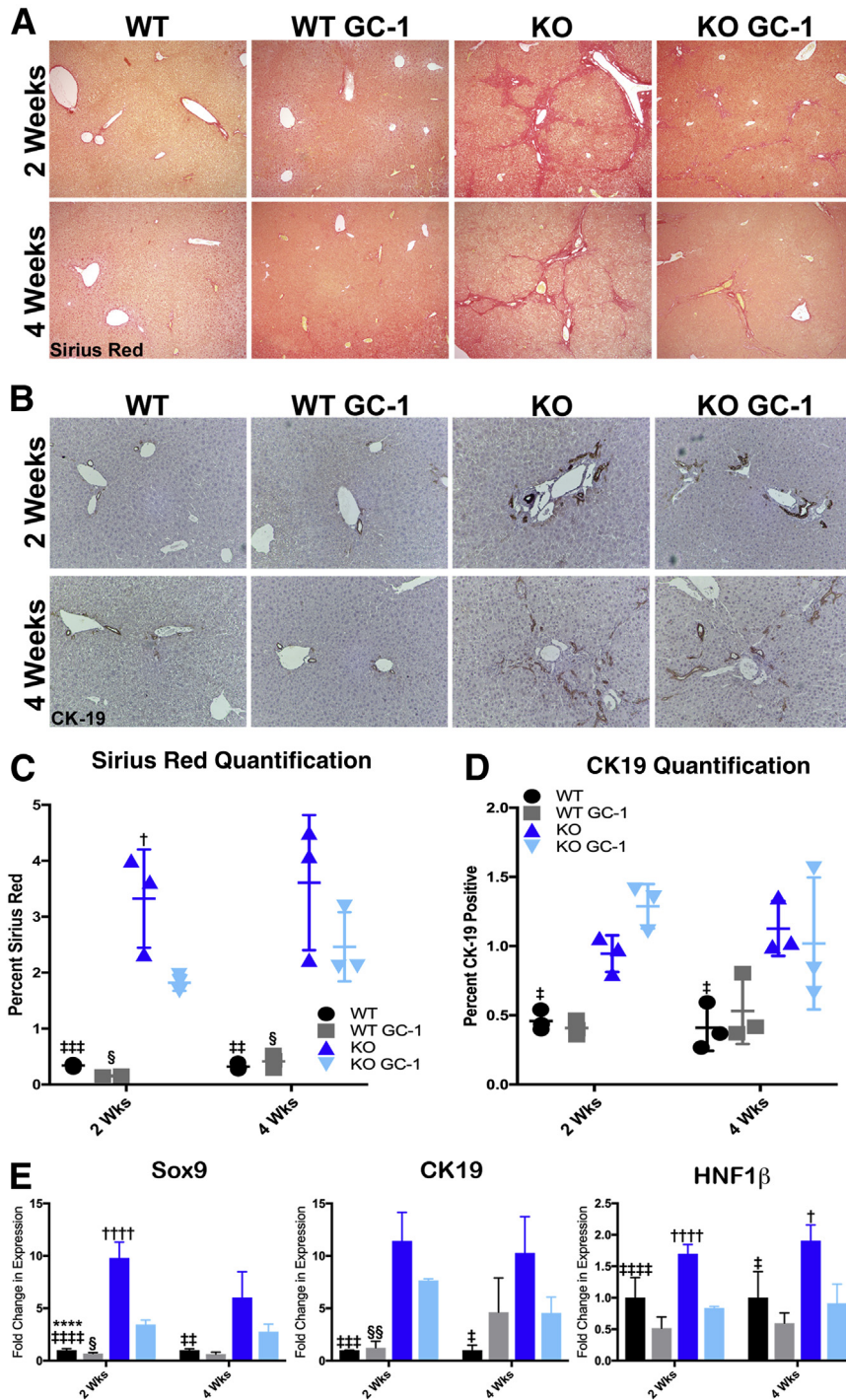
Figure 2 ATP binding cassette subfamily B member 4 ($Abcb4^{-/-}$; Mdr2$^{-/-}$) knockout (KO) mice treated with GC-1 have decreased liver fibrosis but similar ductular response compared with KO mice on normal diet. **A** and **B:** Representative Sirius Red (**A**) and cytokeratin 19 (CK19; **B**) images. **C:** Quantification of Sirius Red stain shows less fibrosis in KO mice of GC-1 diet compared with KO mice after 2 weeks on diet. **D:** Quantification of CK19 shows that KO mice both on and off GC-1 diet have increased ductular response compared with wild-type (WT) mice after 2 and 4 weeks. **E:** Quantitative RT-PCR analysis of cholangiocyte markers sex-determining region Y-box transcription factor 9 (Sox9), CK19, and hepatocyte nuclear factor 1 homeobox B (HNF1β) in WT mice, WT mice fed GC-1 diet, KO mice, and KO mice fed GC-1 diet for 2 and 4 weeks shows decreased expression of these markers in KO treated with GC-1. $n = 3$ mice per group (**E**). ****$P < 0.0001$ WT versus WT GC-1; $^{†}P < 0.05$, $^{††††}P < 0.0001$ KO versus KO GC-1; $^{‡}P < 0.05$, $^{‡‡}P < 0.01$, $^{‡‡‡}P < 0.001$, and $^{‡‡‡‡}P < 0.0001$ WT versus KO; $^{§}P < 0.05$, $^{§§}P < 0.01$ WT GC-1 versus KO GC-1. Original magnification: ×100 (**A**); ×200 (**B**).

by a reduction in serum ALP, but was comparable in KO with and without diet at 12 weeks. To investigate parenchymal injury, hematoxylin and eosin stains of liver sections were performed. KO mice fed GC-1 diet show equivalent portal damage, including inflammation and ductular reaction, as early as 2 weeks compared with KO mice on normal diet, with this trend following into 4 weeks as well (Figure 1B). Thus, despite a transient decrease in biliary injury, KO mice treated

with GC-1 have an overall similar phenotype to KO on normal diet after long-term exposure.

Fibrosis and Ductular Response Are Equivalent in KO Mice Fed GC-1

To determine if lower ALP levels in KO with GC-1 at 2 and 4 weeks correlate with decreased ductular mass and portal
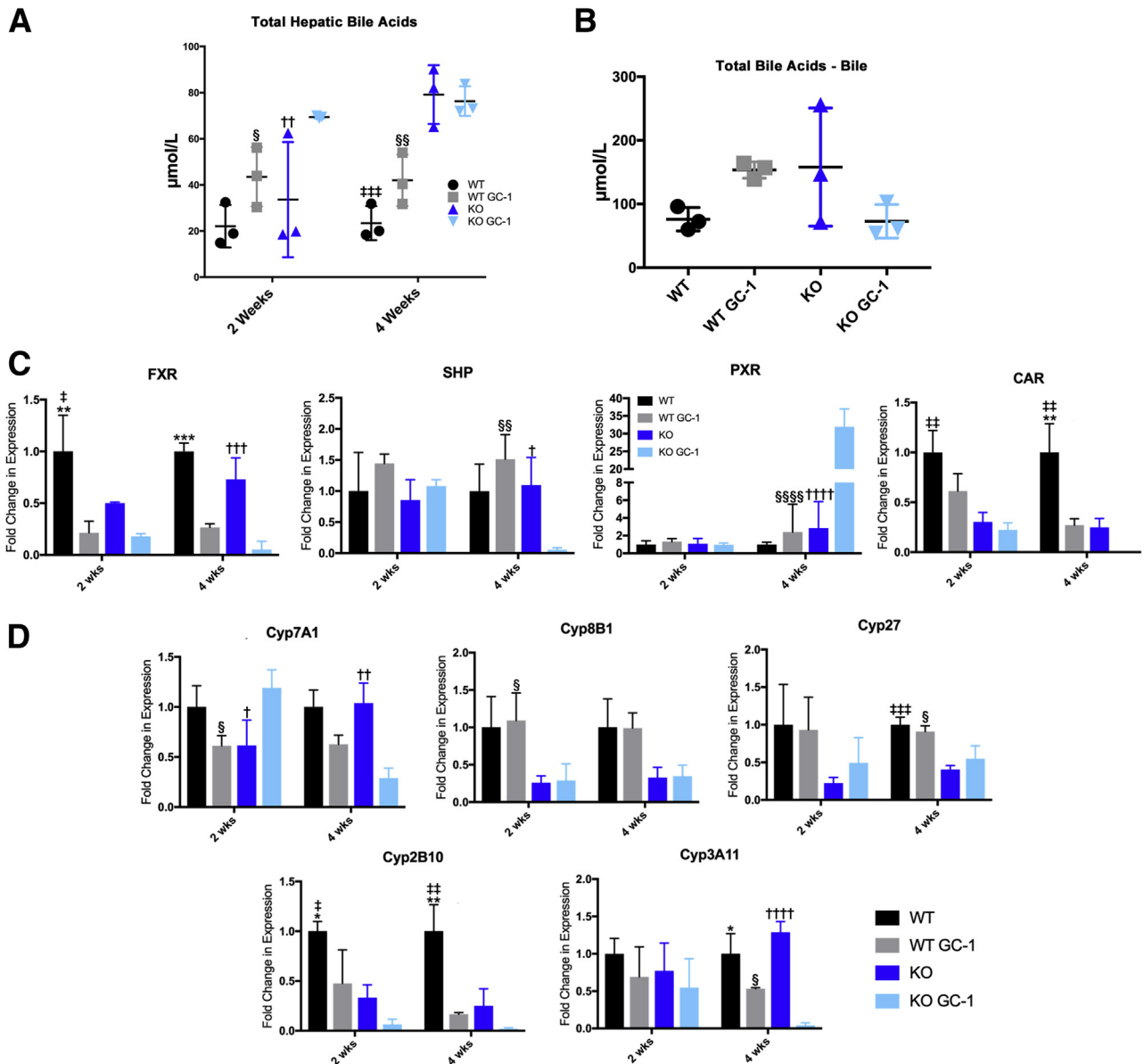
Figure 3 Bile acid excretion is dysregulated in ATP binding cassette subfamily B member 4 ($Abcb4^{-/-}$; $Mdr2^{-/-}$) knockout (KO) mice on GC-1 diet, concomitant with altered nuclear receptor and cytochrome P450 (Cyp) gene expression. **A:** Total hepatic bile acids are increased in KO mice on GC-1 diet after 2 weeks compared with KO controls, but after 4 weeks, bile acid retention in the liver of KO on GC-1 is similar to KO on normal diet. **B:** Measurement of bile acids collected from the gallbladder shows a trend toward decreased bile excretion in KO after 4 weeks of GC-1. **C:** Quantitative RT-PCR analysis of farnesoid X receptor (FXR), small heterodimer partner (SHP), pregnane X receptor (PXR), and constitutive androstane receptor (CAR) shows that, after GC-1 diet, both wild-type (WT) and KO mice have decreased FXR, whereas after 4 weeks of diet, KO mice have increased PXR and decreased SHP; CAR is decreased generally in KO with and without diet. **D:** Bile acid synthesis gene Cyp family 7 subfamily A member 1 ($Cyp7a1$) is increased in KO + GC-1 at 2 weeks, but repressed in KO after 4 weeks of GC-1 treatment, whereas Cyp family 8 subfamily B member 1 ($Cyp8B1$) and Cyp family 27 ($Cyp27$) are decreased in KO irrespective of GC-1 treatment. Detoxification genes Cyp family 3 subfamily a polypeptide 11 ($Cyp3a11$) and Cyp family 2 subfamily b polypeptide 10 ($Cyp2b10$) decreased in both WT and KO after 4 weeks of GC-1. $n = 3$ mice per group (**A–D**). $*P < 0.05$, $**P < 0.01$, and $***P < 0.001$ WT versus WT GC-1; $^{†}P < 0.05$, $^{††}P < 0.01$, $^{†††}P < 0.001$, and $^{††††}P < 0.0001$ KO versus KO GC-1; $^{‡}P < 0.05$, $^{‡‡}P < 0.01$, and $^{‡‡‡}P < 0.001$ WT versus KO; $^{§}P < 0.05$, $^{§§}P < 0.01$, and $^{§§§§}P < 0.0001$ WT GC-1 versus KO GC-1.

fibrosis, the fibrotic content of these livers was assessed by Sirius Red staining and quantification. KO mice on GC-1 diet have significantly less portoportal bridging fibrosis after 2 weeks of diet exposure compared with KO mice, and a trend toward decreased fibrosis at 4 weeks (Figure 2, A and C). Quantitative PCR analysis of biliary markers *Sox9*, cytokeratin 19 (official name *Krt19*), and hepatocyte nuclear

factor 1 homeobox B (official name *Hnf1b*) shows that expression of common cholangiocyte markers is also decreased in KO mice on GC-1 compared with KO mice alone at both 2 and 4 weeks (Figure 2E). Immunohistochemistry for Sox9, however, indicates that the reduction in biliary markers may be due to notably fewer hepatocytes expressing biliary markers after GC-1 compared with KO
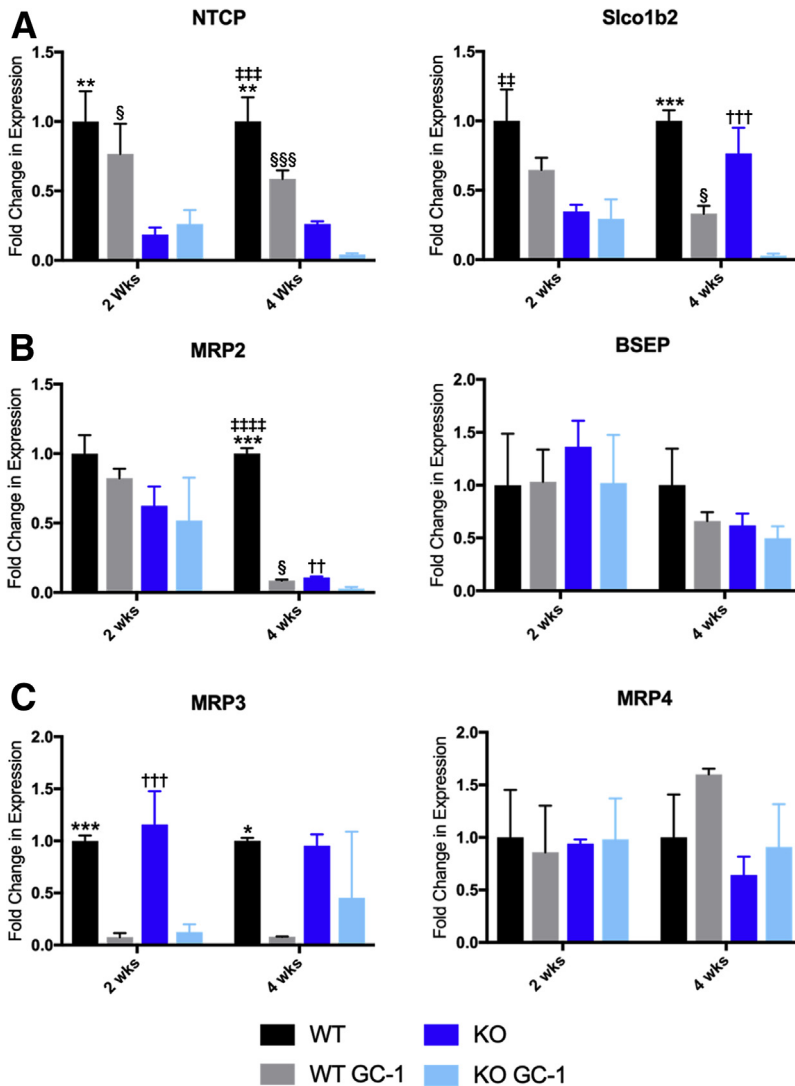
Figure 4 Bile acid transporter genes are altered after GC−1 diet, which leads to toxic bile retention in hepatocytes. **A:** Quantitative RT-PCR analysis of uptake transporters sodium/taurocholate cotransporting polypeptide (*NTCP*) and solute carrier organic anion transporter family, member 1b2 (*Slco1b2*), shows decreased expression in wild-type (WT) and knockout (KO) after 4 weeks of GC-1 diet, although both are suppressed in KO on normal diet as well. **B:** Efflux transporter ATP binding cassette subfamily C member 2 gene [*Abcc2*; alias multidrug resistance protein 2 (MRP2)] is decreased at 4 weeks in both WT and KO on GC-1 compared with controls, whereas bile salt export pump (*BSEP*) is unchanged. **C:** ATP binding cassette subfamily C member 3 (*Abcc3*; alias MRP3) is significantly repressed in both WT and KO on GC-1 at 2 and 4 weeks, whereas ATP binding cassette subfamily C member 4 (*Abcc4*; alias MRP4) is unchanged. $n = 3$ mice per group (**A–C**). $*P < 0.05$, $**P < 0.01$, and $***P < 0.001$ versus WT GC-1; $^{††}P < 0.01$, $^{†††}P < 0.001$ versus KO GC-1; $^{‡‡}P < 0.01$, $^{‡‡‡}P < 0.001$, and $^{‡‡‡‡}P < 0.0001$ versus KO; $^{§}P < 0.05$, $^{§§§}P < 0.001$ GC-1 versus KO GC-1.

mice on normal diet (Supplemental Figure S3), rather than a reduction in the number of biliary structures. To directly assess biliary mass in KO after GC-1, immunohistochemistry and quantification of CK19, a marker of fully differentiated cholangiocytes, were performed. No significant differences in the amount of CK19 positivity between KO with or without GC-1 at either 2 or 4 weeks was observed (Figure 2, B and D). It is concluded that although fibrosis is transiently decreased in KO after 2 weeks of diet, on the whole, neither fibrosis nor ductular response is significantly changed over time in response to GC-1.

GC-1 Alters the Amount and Location of BAs in Mdr2 KO Mice through Differential Regulation of Hepatic BA Transporters and Synthesis Enzymes

Despite insignificant differences during the 12-week time point, this study intended to further characterize the phenotype of KO mice at the early stage of GC-1 treatment.

Because hepatic injury increases simultaneously with decreased biliary injury in KO fed GC-1, it is hypothesized that alterations in BA synthesis, detoxification, or transport may be responsible.

Measurement of BAs shows that KO mice on GC-1 for 2 weeks have higher total hepatic BAs compared with both KO on normal diet and WT mice on GC-1 (Figure 3A). However, at 4 weeks, KO mice with and without GC-1 have similar levels of hepatic BAs, which are both elevated compared with WT mice (Figure 3A). At 4 weeks, a trend was also noted toward decrease in BA excretion, as KO fed GC-1 for 4 weeks have decreased biliary (gallbladder) BA levels compared with KO alone (Figure 3B). Thus, by 4 weeks, KO have compensated for increased BA accumulation after GC-1 by altering the amount and location of BA in the liver.

Quantitative PCR analysis was then used to determine if nuclear receptors associated with BA synthesis—farnesoid X receptor [FXR; alias nuclear receptor subfamily 1 group
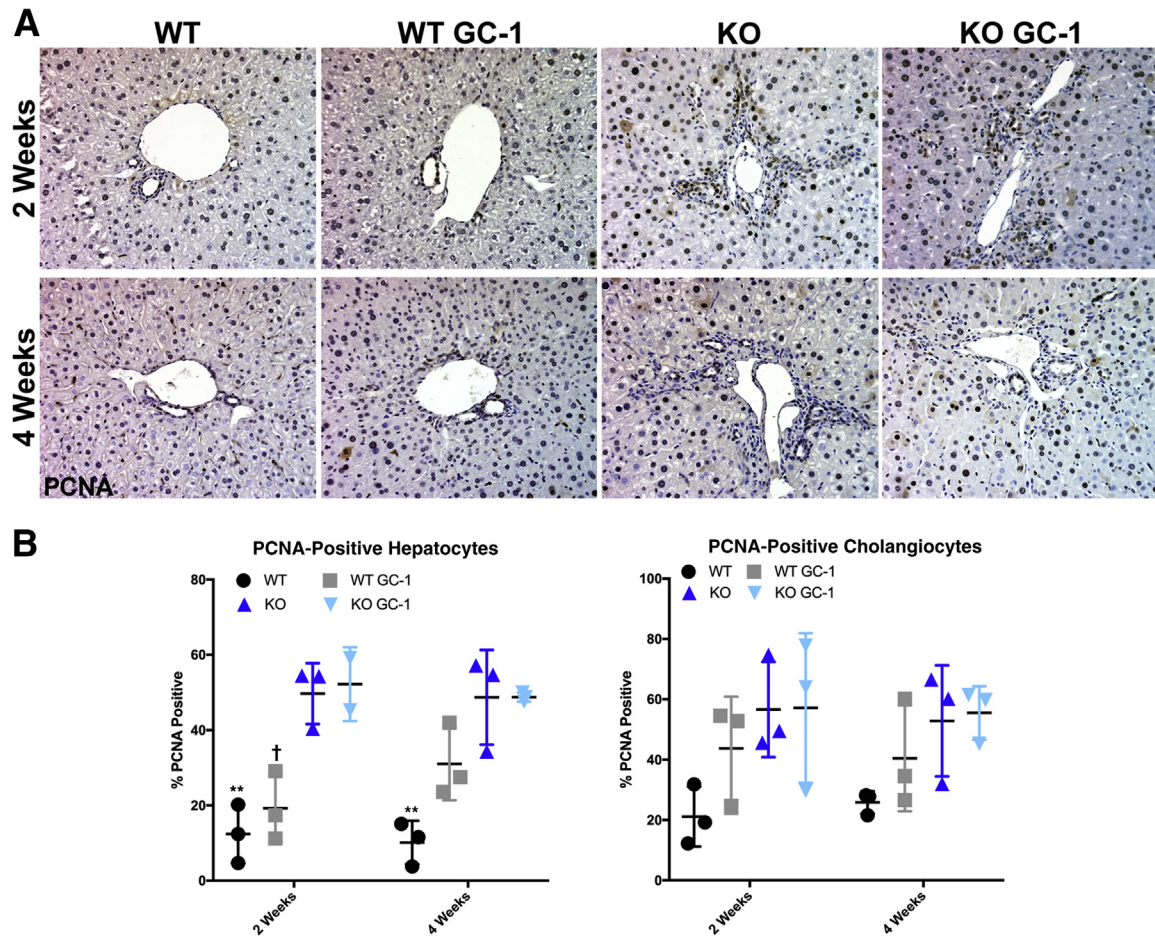
Figure 5 GC-1 has no effect on either hepatocyte or cholangiocyte proliferation in ATP binding cassette subfamily B member 4 (*Abcb4*^{−/−}; Mdr2^{−/−}) knockout (KO) mice. **A:** Representative proliferating cell nuclear antigen (PCNA) images. **B:** PCNA quantification shows that hepatocyte proliferation increases after GC-1 in wild type (WT) and increases significantly between WT and KO, but not between KO and KO + GC-1. Cholangiocyte proliferation in livers of KO mice fed GC-1 diet is also comparable to mice fed normal diet. **P < 0.01 versus WT GC-1; †P < 0.05 versus KO GC-1. Original magnification, ×200 (**A**).

H member 4 (*Nr1h4*)], small heterodimer partner [alias nuclear receptor subfamily 0 group B member 2 (*Nr0b2*)], pregnane X receptor [alias nuclear receptor subfamily 1 group I member 2 (*Nr1i2*)], and constitutive androstane receptor [alias coxsackie virus and adenovirus receptor Ig-like cell adhesion molecule (*Cxadr*)]—were altered after GC-1 exposure. FXR and its downstream target small heterodimer partner are master regulators of BA synthesis, whereas pregnane X receptor and constitutive androstane receptor regulate expression of cytochrome P450 (Cyp) genes involved in detoxifying and transporting BAs.[19,20] This study found that GC-1 reduced expression of FXR after 2 and 4 weeks of treatment, a finding that was consistent across both genotypes (Figure 3C). On the other hand, only KO show a decrease in small heterodimer partner after 4 weeks of GC-1 exposure, despite similar expression levels to WT at 2 weeks. Interestingly, expression of pregnane X receptor is dramatically increased in KO after 4 weeks of GC-1 diet, whereas constitutive androstane receptor expression is suppressed in KO generally, and GC-1 decreases expression further at 4 weeks (Figure 3C).

Thus, the disparate regulation of some nuclear receptors, with the exception of FXR, indicates a compensatory response to GC-1 that is exclusive to KO.

To determine the impact on BA synthesis and detoxification, the expression of the Cyps involved in these processes was next analyzed. Interestingly, Cyp7a1, the rate-limiting enzyme involved in BA synthesis from cholesterol, is induced in KO mice on GC-1 for 2 weeks compared with KO mice, but significantly suppressed after 4 weeks of GC-1 exposure; expression in WT is unchanged at either time point after GC-1 (Figure 3D). Cyp8b1, which is downstream of Cyp7a1 and synthesizes cholic acid, is suppressed in the KO mice regardless of GC-1 treatment. Likewise, Cyp27, which initiates the alternative BA synthesis pathway, is decreased in KO at both 2 and 4 weeks. Finally, expression of Cyp3a11 and Cyp2b10, which are involved in BA detoxification, significantly decreases after GC-1 diet in both WT and KO mice (Figure 4C). The results show that alternations in BA synthesis and detoxification occur early after GC-1 treatment, and may subsequently affect both BA levels and toxicity.
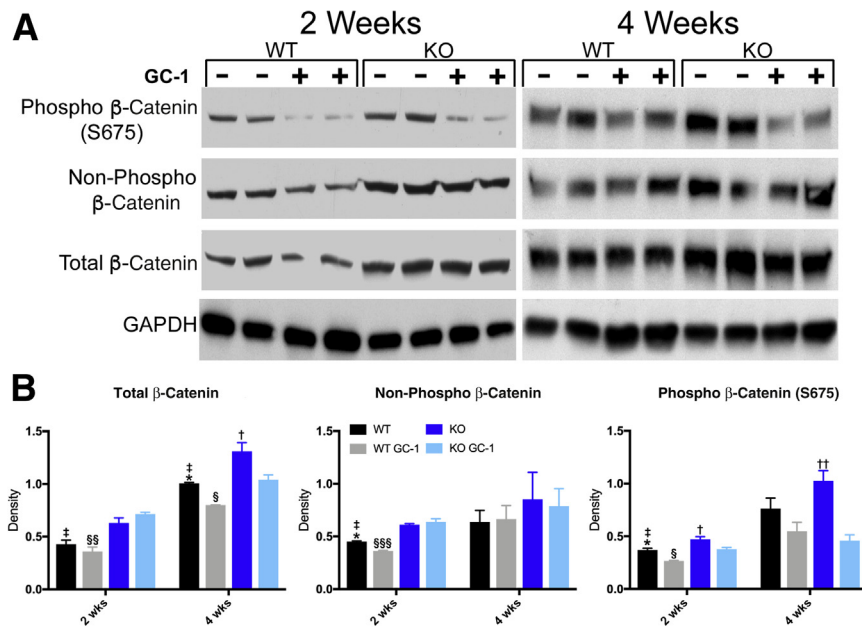
Figure 6 β-Catenin is not activated by GC-1 in ATP binding cassette subfamily B member 4 (Abcb4^−/−; Mdr2^−/−) knockout (KO) mice. Western blot analyses (**A**) and densitometry of the Western blot analyses (**B**) for phosphorylated (S675), nonphosphorylated active, and total β-catenin shows that KO mice given GC-1 have decreased activation of phosphorylated (S675) β-catenin compared with KO mice. *P < 0.05 versus WT GC-1; †P < 0.05, ††P < 0.01 versus KO GC-1; ‡P < 0.05 versus KO; §P < 0.05, §§P < 0.01, and §§§P < 0.001 versus KO GC-1. GAPDH, glyceraldehyde-3-phosphate dehydrogenase; phospho, phosphorylated; WT, wild-type.

Finally, the expression of genes involved in BA transport to identify any dysregulation in the presence of GC-1 was analyzed. Bile acid uptake transporters sodium-taurocholate cotransporting polypeptide [alias solute carrier family 10 member 1 (Slc10a1)] and solute carrier organic anion transporter family, member 1b2 [Slco1b2; (Slo)1b2], which are already decreased in KO mice compared with WT, are further reduced in both WT and KO after 4 weeks of GC-1 (Figure 4A). Expression of apical BA efflux transporter, ATP binding cassette subfamily C member 2 [Abcc2; alias multidrug resistance protein 2 (MRP2)], is decreased in both WT and KO, albeit only after 4 weeks of GC-1, whereas the bile salt export pump, another efflux transporter, is unchanged between WT and KO with or without GC-1 at either time point (Figure 4B). Decreased expression of MRP3, a basolateral BA efflux transporter, officially known as ATP binding cassette subfamily C member 3 (Abcc3), is also seen in both WT and KO at 2 and 4 weeks, indicating a direct repression by GC-1, whereas MRP4, another basolateral transporter officially known as ATP binding cassette subfamily C member 4 (Abcc4), is unchanged (Figure 4C). Overall, GC-1 induces down-regulation of FXR, BA uptake and efflux transporters, and detoxification enzymes in both WT and KO, with net result being that hepatocytes retain more toxic BAs compared with hepatocytes from mice on normal diet (Supplemental Figure S4). However, KO mice on GC-1 also show increased Cyp7a1 expression at 2 weeks, which may account for the elevated levels of BAs and increased hepatic damage at this time point.

GC-1 Neither Induces Hepatocyte Proliferation nor Inhibits Cholangiocyte Proliferation in Mdr2 KO Mice

Hepatocyte proliferation is an important component of the reparative response in chronic liver injury, and is often deficient in patients with cholestasis.[21–24] As GC-1 has been shown to have mitogenic effects on hepatocytes, specifically after partial hepatectomy, the cell proliferation in our model was analyzed.[15] Quantification of proliferating cell nuclear antigen immunohistochemistry shows increased hepatocyte proliferation in WT mice administered GC-1, as expected (Figure 5). However, hepatocyte proliferation in Mdr2 KO mice on normal diet, which was significantly elevated compared with WT, was not further induced by GC-1. A previous study has also found that thyroid hormone inhibits biliary growth both in vitro and in vivo, suggesting a cell autonomous role of thyroid receptor activation in cholangiocyte proliferation.[25] However, neither WT nor KO mice exposed to GC-1 diet had any significant changes in cholangiocyte proliferation compared with mice fed normal diet (Figure 5). Thus, GC-1 diet does not affect proliferation of cholangiocytes, and hepatocyte proliferation is increased in WT but not Mdr2 KO after GC-1.

GC-1 Does Not Activate β-Catenin in Mdr2 KO Mice

As the effect of GC-1 on hepatocyte proliferation is β-catenin dependent, a Western blot analysis of key phosphorylation sites that regulate β-catenin activation was performed. Previous studies have shown that GC-1 increases phosphorylation of β-catenin at serine 675.[15] However, KO mice fed GC-1 diet have decreased S675 phosphorylated β-catenin after 2 and 4 weeks of diet exposure compared with KO mice on normal diet (Figure 6). This decrease in S675 phosphorylated β-catenin indicates that the changes seen in the KO mice on GC-1 compared with the KO mice are not driven by protein kinase A−dependent β-catenin activation. To determine if GC-1 induces activation of β-catenin through canonical Wnt signaling, an antibody against the
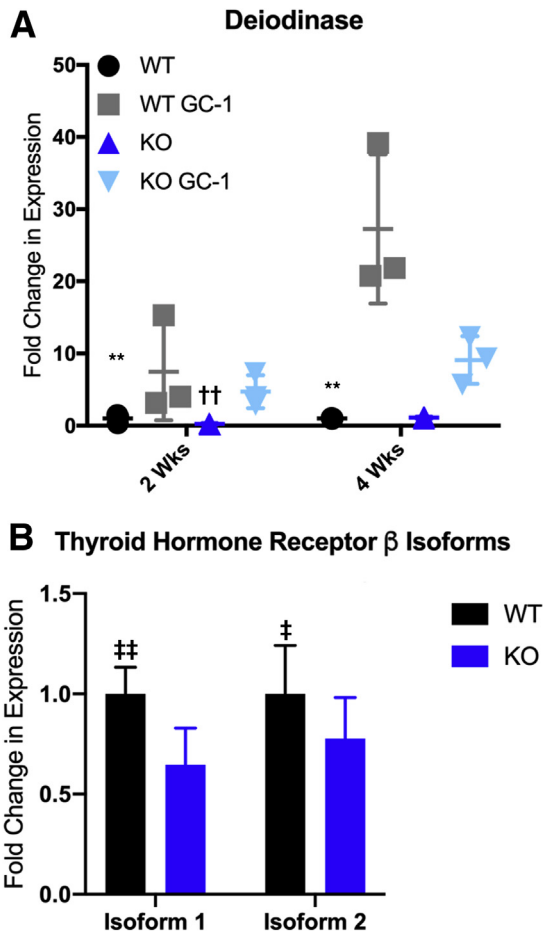
Figure 7 GC-1 induces deiodinase expression to a lesser extent in ATP binding cassette subfamily B member 4 (*Abcb4*$^{-/-}$; Mdr2$^{-/-}$) knockout (KO) livers than in wild-type (WT) livers, due to decreased expression of thyroid hormone receptor β (TRβ) receptor. **A:** Quantitative RT-PCR analysis of deiodinase expression shows that KO have decreased induction after 2 and 4 weeks of GC-1 diet compared with WT mice ($P < 0.01$). **B:** Expression of the two common isoforms of TRβ is decreased in baseline KO mice compared with baseline WT mice. $n \geq 3$ mice per group (**A**). **$P < 0.01$ versus WT GC-1; $^{\dagger\dagger}P < 0.01$, $^{\dagger\dagger\dagger}P < 0.001$ versus KO GC-1; $^{\ddagger}P < 0.05$, $^{\ddagger\ddagger}P < 0.01$ versus KO.

hypophosphorylated (nonphosphorylated) form of β-catenin was used. No significant changes in Wnt-dependent β-catenin activation were observed in KO treated with GC-1 at either the 2- or 4-week time point, although β-catenin activation was increased in KO livers compared with WT, as shown previously.[10]

TRβ Expression Is Decreased in Mdr2 KO, Resulting in a Blunted Response to GC-1

The lack of β-catenin activation led us to question whether GC-1 was being efficiently taken up and metabolized by the liver. This study sought to verify the effectiveness of GC-1 by examining expression of deiodinase, which is a TRβ target gene. Interestingly, although deiodinase is significantly up-regulated in WT, particularly at 4 weeks (approximately 30-fold over control), expression is

increased only approximately 10-fold in KO after 4 weeks (Figure 7A). The study then analyzed the expression of the two TRβ isoforms in both WT and KO, and found that both were decreased in KO compared with WT at baseline (Figure 7B). Thus, GC-1 may be less effective in inducing β-catenin activation and hepatocyte proliferation in KO because of down-regulation of the receptors that interact with this thyroid hormone analog.

Discussion

There is some evidence that activation of the Wnt/β-catenin signaling pathway may be protective in a subset of patients with cholestatic liver disease. Transgenic mice expressing a mutated, nondegradable form of β-catenin had decreased ALP, which is commonly used to monitor response to treatment in PSC patients, after long-term treatment with 5-diethoxycarbonyl-1,4-dihydrocollidine.[26] Mdr2 KO mice also required β-catenin activation for maintenance of homeostasis.[10] Because TRβ agonist was shown to activate β-catenin, it is hypothesized that administration of GC-1 might alleviate injury in the Mdr2 KO mouse. However, only a modest decrease in biliary injury and fibrosis in KO mice given GC-1, which was restricted to early (2- and 4-week) time points, was observed. The improvement in injury was not due to increased hepatocyte proliferation and repair, but rather a decrease in the amount of toxic bile entering the biliary tree.

Despite decreased biliary injury, however, KO showed a significant increase in hepatic injury, as assessed by serum aspartate aminotransferase and alanine transaminase as well as apoptosis. Notably, serum ALP, aspartate aminotransferase, and alanine transaminase levels also increased in WT mice treated with GC-1. Interestingly, patients with familial hypercholesterolemia taking another thyroid hormone mimetic, KB2115, also showed a dose-dependent increase in transaminases and conjugated bilirubin.[27] It is unknown whether these effects were off target or due to the effect of mimicking thyrotoxicosis in the liver; nonetheless, they are consistent with previous findings and led to discontinuation of treatment in some cases.[27]

The pathogenesis of injury in Mdr2 KO is complex and multifactorial; however, increased concentration of free toxic BAs in the biliary tree is one major contributor. One strategy to reduce bile toxicity is to decrease BA output, which can be accomplished by treating these mice with the dual FXR and G-protein–coupled membrane BA receptor (TGR5) agonist INT767.[28] In this study, GC-1 treatment of KO led to higher BA levels in the liver but lower levels in gallbladder bile than WT or KO on normal diet, resulting in less biliary injury. It appears that GC-1 causes retention of BAs in hepatocytes, thus sparing cholangiocytes from injury (Figure 7A). Indeed, GC-1 has important roles in lipid metabolism, including promoting conversion of cholesterol into BAs and regulating secretion of cholesterol into bile.[29,30]

It was intriguing to note that GC-1 enhanced BA toxicity and decreased their export. Increased toxicity occurs because of down-regulation of Cyp2b10 (and eventually Cyp3a11). The increase in Cyp7a1 in KO on GC-1 at 2 weeks, despite simultaneous decreases in Cyp8b1 and Cyp27, likely leads to additional BA accumulation and increased total hepatic BA levels in these mice. Alternative export of BAs from the basolateral membrane is suppressed at both 2 and 4 weeks of diet in both WT and KO by GC-1, as is export from the apical side at 4 weeks. The down-regulation of BA uptake transporters from the blood is likely a secondary effect of the increasing levels of hepatic BAs, particularly in the KO. We believe that, although collectively these changes due to GC-1 result in increased biliary injury in WT due to the increased toxicity of bile, they induce hepatic injury in KO, because the toxic BAs are accumulating in hepatocytes rather than being dumped into bile. Future studies will address if some of these effects of GC-1 are indirect because of impact on cholesterol metabolism.[31]

GC-1 led to an unexpected decrease in β-catenin expression and activity in Mdr2 KO. A previous study had shown GC-1 to activate both Wnt-dependent and Wnt-independent (protein kinase A—mediated Ser675 phosphorylation) activation of β-catenin.[15] However, both the mode of GC-1 delivery and the length of treatment differed between the two studies, which may explain the conflicting results. The liver regeneration studies used mice injected with GC-1 for up to 8 days and harvested 1 hour after the final injection, which would allow for accurate measurement of transient events, such as protein phosphorylation. Conversely, in this study, mice consumed GC-1—containing diet ad libitum for a much longer time period (2 and 4 weeks), and were sacrificed without fasting. These conditions may not have been optimal for assessing phosphorylation events, as these are highly temporal within a cell.

Furthermore, TRβ expression was suboptimal in KO. It is possible that chronic liver injury may induce hepatocyte dedifferentiation, and decreased TRβ expression occurs as a result of this reprogramming. Thus, although compensatory hepatocyte proliferation in the Mdr2 KO likely occurs as a response to tissue damage, and may provide some protection against chronic injury,[32] these cells are less responsive to therapies, such as thyromimetics, which rely on the presence of receptors expressed in fully differentiated hepatocytes. Further studies are needed to investigate the efficacy of thyromimetics in cholestatic models like Mdr2 KO after forced expression of TRβ.

Interestingly, a recent article demonstrated TRβ agonists to increase Mdr2 expression transcriptionally.[33] This promoted phosphatidylcholine secretion into the bile, increasing bile flow and biliary BA output. It is unclear whether this is a reciprocal relationship, with down-regulation of Mdr2 leading to decreased TRβ, but these results suggest that this may be the case. Nonetheless, although the effect on Mdr2 induction was not tested in mouse models of cholestasis, *in vitro* studies using T3 and an FXR agonist showed that the effects of combination therapy are additive, resulting in stimulation of Mdr2 expression and sustained repression of Cyp7a1.[33] This study demonstrates that reducing exposure of the biliary system to toxic BAs has an overall beneficial effect, and that the combination of TRβ agonists with other therapeutic modalities, such as FXR agonists, may be synergistic in reducing accumulation of BAs in hepatocytes and subsequent hepatic injury. More optimization of TRβ expression would be necessary to test this hypothesis, but because thyromimetics are already undergoing preclinical and clinical trials, these findings have important implications for drug repurposing and personalized medicine.

Acknowledgment

Supplemental Data

Supplemental material for this article can be found at *http://doi.org/10.1016/j.ajpath.2020.01.015*.

References

1. Karlsen TH, Folseraas T, Thorburn D, Vesterhus M: Primary sclerosing cholangitis: a comprehensive review. J Hepatol 2017, 67: 1298—1323
2. Dyson JK, Beuers U, Jones DEJ, Lohse AW, Hudson M: Primary sclerosing cholangitis. Lancet 2018, 391:2547—2559
3. Lazaridis KN, LaRusso NF: Primary sclerosing cholangitis. N Engl J Med 2016, 375:1161—1170
4. Fickert P, Fuchsbichler A, Wagner M, Zollner G, Kaser A, Tilg H, Krause R, Lammert F, Langner C, Zatloukal K, Marschall HU, Denk H, Trauner M: Regurgitation of bile acids from leaky bile ducts causes sclerosing cholangitis in Mdr2 (Abcb4) knockout mice. Gastroenterology 2004, 127:261—274
5. Smit JJ, Schinkel AH, Oude Elferink RP, Groen AK, Wagenaar E, van Deemter L, Mol CA, Ottenhoff R, van der Lugt NM, van Roon MA, van der Valk MA, Offerhaus GJ, Berns AJ, Borst P: Homozygous disruption of the murine mdr2 P-glycoprotein gene leads to a complete absence of phospholipid from bile and to liver disease. Cell 1993, 75:451—462
6. Fickert P, Pollheimer MJ, Beuers U, Lackner C, Hirschfield G, Housset C, Keitel V, Schramm C, Marschall HU, Karlsen TH, Melum E, Kaser A, Eksteen B, Strazzabosco M, Manns M, Trauner M; International PSC Study Group (IPSCSG): Characterization of animal models for primary sclerosing cholangitis (PSC). J Hepatol 2014, 60:1290—1303
7. Monga SP: Beta-catenin signaling and roles in liver homeostasis, injury, and tumorigenesis. Gastroenterology 2015, 148:1294—1310
8. Thompson MD, Moghe A, Cornuet P, Marino R, Tian J, Wang P, Ma X, Abrams M, Locker J, Monga SP, Nejak-Bowen K: Beta-catenin regulation of farnesoid X receptor signaling and bile acid metabolism during murine cholestasis. Hepatology 2018, 67: 955—971

9. Saggi H, Maitra D, Jiang A, Zhang R, Wang P, Cornuet P, Singh S, Locker J, Ma X, Dailey H, Abrams M, Omary MB, Monga SP, Nejak-Bowen K: Loss of hepatocyte beta-catenin protects mice from experimental porphyria-associated liver injury. J Hepatol 2019, 70: 108−117

10. Pradhan-Sundd T, Kosar K, Saggi H, Zhang R, Vats R, Cornuet P, Green S, Singh S, Zeng G, Sundd P, Nejak-Bowen K: Wnt/beta-catenin signaling plays a protective role in the Mdr2 KO murine model of cholestatic liver disease. Hepatology 2019, [Epub ahead of print] doi:10.1002/hep.30927

11. Kowalik MA, Perra A, Pibiri M, Cocco MT, Samarut J, Plateroti M, Ledda-Columbano GM, Columbano A: TRbeta is the critical thyroid hormone receptor isoform in T3-induced proliferation of hepatocytes and pancreatic acinar cells. J Hepatol 2010, 53:686−692

12. Ledda-Columbano GM, Molotzu F, Pibiri M, Cossu C, Perra A, Columbano A: Thyroid hormone induces cyclin D1 nuclear translocation and DNA synthesis in adult rat cardiomyocytes. FASEB J 2006, 20:87−94

13. Gullberg H, Rudling M, Salto C, Forrest D, Angelin B, Vennstrom B: Requirement for thyroid hormone receptor beta in T3 regulation of cholesterol metabolism in mice. Mol Endocrinol 2002, 16: 1767−1777

14. Fanti M, Singh S, Ledda-Columbano GM, Columbano A, Monga SP: Tri-iodothyronine induces hepatocyte proliferation by protein kinase A-dependent beta-catenin activation in rodents. Hepatology 2014, 59: 2309−2320

15. Alvarado TF, Puliga E, Preziosi M, Poddar M, Singh S, Columbano A, Nejak-Bowen K, Monga SP: Thyroid hormone receptor beta agonist induces beta-catenin-dependent hepatocyte proliferation in mice: implications in hepatic regeneration. Gene Expr 2016, 17:19−34

16. Chiellini G, Apriletti JW, Yoshihara HA, Baxter JD, Ribeiro RC, Scanlan TS: A high-affinity subtype-selective agonist ligand for the thyroid hormone receptor. Chem Biol 1998, 5:299−306

17. Thompson MD, Wickline ED, Bowen WB, Lu A, Singh S, Misse A, Monga SP: Spontaneous repopulation of beta-catenin null livers with beta-catenin-positive hepatocytes after chronic murine liver injury. Hepatology 2011, 54:1333−1343

18. Schindelin J, Arganda-Carreras I, Frise E, Kaynig V, Longair M, Pietzsch T, Preibisch S, Rueden C, Saalfeld S, Schmid B, Tinevez JY, White DJ, Hartenstein V, Eliceiri K, Tomancak P, Cardona A: Fiji: an open-source platform for biological-image analysis. Nat Methods 2012, 9:676−682

19. Goodwin B, Jones SA, Price RR, Watson MA, McKee DD, Moore LB, Galardi C, Wilson JG, Lewis MC, Roth ME, Maloney PR, Willson TM, Kliewer SA: A regulatory cascade of the nuclear receptors FXR, SHP-1, and LRH-1 represses bile acid biosynthesis. Mol Cell 2000, 6:517−526

20. Guo GL, Lambert G, Negishi M, Ward JM, Brewer HB Jr, Kliewer SA, Gonzalez FJ, Sinal CJ: Complementary roles of farnesoid X receptor, pregnane X receptor, and constitutive androstane receptor in protection against bile acid toxicity. J Biol Chem 2003, 278:45062−45071

21. Georgiev P, Jochum W, Heinrich S, Jang JH, Nocito A, Dahm F, Clavien PA: Characterization of time-related changes after experimental bile duct ligation. Br J Surg 2008, 95:646−656

22. Bai H, Zhang N, Xu Y, Chen Q, Khan M, Potter JJ, Nayar SK, Cornish T, Alpini G, Bronk S, Pan D, Anders RA: Yes-associated protein regulates the hepatic response after bile duct ligation. Hepatology 2012, 56:1097−1107

23. van Golen RF, Olthof PB, Lionarons DA, Reiniers MJ, Alles LK, Uz Z, de Haan L, Ergin B, de Waart DR, Maas A, Verheij J, Jansen PL, Damink SWO, Schaap FG, van Gulik TM, Heger M: FXR agonist obeticholic acid induces liver growth but exacerbates biliary injury in rats with obstructive cholestasis. Sci Rep 2018, 8:16529

24. Yokoyama Y, Nagino M, Nimura Y: Mechanism of impaired hepatic regeneration in cholestatic liver. J Hepatobiliary Pancreat Surg 2007, 14:159−166

25. Fava G, Ueno Y, Glaser S, Francis H, DeMorrow S, Marucci L, Marzioni M, Benedetti A, Venter J, Vaculin B, Vaculin S, Alpini G: Thyroid hormone inhibits biliary growth in bile duct-ligated rats by PLC/IP3/Ca2+-dependent downregulation of SRC/ERK1/2. Am J Physiol Cell Physiol 2007, 292:C1467−C1475

26. Thompson MD, Awuah P, Singh S, Monga SP: Disparate cellular basis of improved liver repair in beta-catenin-overexpressing mice after long-term exposure to 3,5-diethoxycarbonyl-1,4-dihydrocollidine. Am J Pathol 2010, 177:1812−1822

27. Sjouke B, Langslet G, Ceska R, Nicholls SJ, Nissen SE, Ohlander M, Ladenson PW, Olsson AG, Hovingh GK, Kastelein JJ: Eprotirome in patients with familial hypercholesterolaemia (the AKKA trial): a randomised, double-blind, placebo-controlled phase 3 study. Lancet Diabetes Endocrinol 2014, 2:455−463

28. Baghdasaryan A, Claudel T, Gumhold J, Silbert D, Adorini L, Roda A, Vecchiotti S, Gonzalez FJ, Schoonjans K, Strazzabosco M, Fickert P, Trauner M: Dual farnesoid X receptor/TGR5 agonist INT-767 reduces liver injury in the Mdr2-/- (Abcb4-/-) mouse cholangiopathy model by promoting biliary HCO(-)(3) output. Hepatology 2011, 54:1303−1312

29. Bonde Y, Plosch T, Kuipers F, Angelin B, Rudling M: Stimulation of murine biliary cholesterol secretion by thyroid hormone is dependent on a functional ABCG5/G8 complex. Hepatology 2012, 56: 1828−1837

30. Gullberg H, Rudling M, Forrest D, Angelin B, Vennstrom B: Thyroid hormone receptor beta-deficient mice show complete loss of the normal cholesterol 7alpha-hydroxylase (CYP7A) response to thyroid hormone but display enhanced resistance to dietary cholesterol. Mol Endocrinol 2000, 14:1739−1749

31. Angelin B, Rudling M: Lipid lowering with thyroid hormone and thyromimetics. Curr Opin Lipidol 2010, 21:499−506

32. De Vree JM, Ottenhoff R, Bosma PJ, Smith AJ, Aten J, Oude Elferink RP: Correction of liver disease by hepatocyte transplantation in a mouse model of progressive familial intrahepatic cholestasis. Gastroenterology 2000, 119:1720−1730

33. Gautherot J, Claudel T, Cuperus F, Fuchs CD, Falguieres T, Trauner M: Thyroid hormone receptor beta1 stimulates ABCB4 to increase biliary phosphatidylcholine excretion in mice. J Lipid Res 2018, 59:1610−1619